THE JOURNAL OF BIOLOGICAL CHEMISTRY VOL. 288, NO. 17, pp. 12130–12141, April 26, 2013

An Allelic Series at the Paired Box Gene 6 (*Pax6*) Locus Reveals the Functional Specificity of *Pax* Genes*

Received for publication, November 16, 2012, and in revised form, March 20, 2013 Published, JBC Papers in Press, March 20, 2013, DOI 10.1074/jbc.M112.436865

Christian Carbe, Ankur Garg, Zhigang Cai, Hongge Li, Andrea Powers, and Xin Zhang[1]

From the Departments of Medical and Molecular Genetics and Biochemistry and Molecular Biology, Indiana University School of Medicine, Indianapolis, Indiana 46202

Background: *Pax6*, *Pax6*(*5a*), and *Pax2* are derived from a common *Pax2*-like ancestral gene.
Results: *Pax6*(*5a*) and *Pax2* can partially substitute for *Pax6* in neural development.
Conclusion: The specificities of *Pax6*(*5a*) and *Pax2* paired domains correspond to the extent of the rescues in forebrain but not in eye development.
Significance: The unique function of *Pax6* in eye development requires the combined activities of paired domain and homeodomain.

The advent of the ocular and nervous system in metazoan evolution coincides with the diversification of a single ancestral paired box (*Pax*) gene into *Pax6*, *Pax6*(*5a*), and *Pax2*. To investigate the role of these *Pax* genes in neural development, we have generated an allelic series of knock-in models at the *Pax6* locus. We showed that although *Pax6*(*5a*) and *Pax2* could not replace *Pax6* for its autoregulation in lens induction or for neural differentiation in retina, *Pax6*(*5a*) was sufficient for corneal-lenticular detachment. In brain development, cell proliferation in the cerebral cortex and dorsoventral patterning of the telencephalon and neural tube were partially rescued in either knock-in mutant. Contrary to the previous belief, our genetic studies showed that the *Pax6* isoform *Pax6*(*5a*) could potentially play a role in neuronal differentiation in brain development. Importantly, *Pax2* showed greater rescue efficiency than *Pax6*(*5a*) in the telencephalon even though the latter was identical to *Pax6* outside the paired domain. In studying *Ngn2*, a *Pax6* direct target gene in telencephalon, we showed that the level of *Ngn2* expression correlated with the *in vitro* binding of Pax2, Pax6, and Pax6(5a) paired domain on its enhancer. Our results show that *Pax6* is uniquely required for eye development, but in brain development, *Pax6* can be functionally substituted by related *Pax* family genes that share a similar paired domain binding specificity.

The *Pax*[2] family of transcription factors is a metazoan innovation that can be traced back evolutionarily to a single *Pax2*-like gene in sponge, which has no eye or nervous system (for a review, see Ref. 1). The emergence of the visual system in bilateria coincides with the separation of *Pax2* and *Pax6* genes, whereas further gene duplications in *Drosophila* resulted in two canonical *Pax6* paralogues (*ey* and *toy*) and two *Pax6*(*5a*)-like genes (*eyg* and *toe*). The importance of *Pax6*, *Pax6*(*5a*), and *Pax2* in *Drosophila* eye development has been clearly demonstrated by the *ey* and the *eyg* mutants, which have no eyes, and by the *Pax2* mutants, which have abnormal cone cells (2–4). It was further shown that *Drosophila Pax6*, *Pax6*(*5a*), and *Pax2* have separate functions with *ey* controlling retinal specification, *eyg* regulating cell growth, and *Pax2* involved in cone and pigment cell development (2, 5). However, the *Pax2* and *Pax6* paired domains share remarkably similar consensus DNA binding sites, and at least in *Drosophila*, the paired domain (PD) but not the homeodomain (HD) of *Pax6* was required for eye development (6). Furthermore, *Pax6*(*5a*), but not *Pax6*, was shown to be able to induce ectopic retina in chick (7). These results raise the question whether *Pax6*, *Pax6*(*5a*), and *Pax2* are functionally exchangeable in mammalian eye development.

Pax6 plays multiple roles in neural development. Humans heterozygous for *PAX6* develop blindness, aniridia, colobomas, and cataracts, whereas *Pax6*-null mice (*Pax6*$^{Sey/Sey}$; small eye) fail to form any mature eye structures (8–11). This is because *Pax6* expression, which appears in the head surface ectoderm prior to lens placode formation, is crucial for lens induction as well as differentiation (12, 13). Although the remaining *Pax6*-null retinal primordia initially up-regulate retina-specific markers, such as Crx for photoreceptor cells and VC1.1 for amacrine cells, the neurogenic program is eventually aborted (14–16). During neural tube development, *Pax6* controls ventral patterning through its antagonistic interaction with *Nkx2.2*, establishing distinct populations of progenitor cells (17). In contrast, *Pax6* expression in forebrain is primarily restricted to the dorsal telencephalon where *Pax6* activates the dorsal telencephalic transcription factor *Ngn2* expression to prevent the expansion of ventral transcription factor *Mash1* while maintaining the boundary structures to restrict cell migration (18, 19). In addition to these neural patterning defects, the *Pax6*-null progenitors in the dorsal telencephalon also present with cell cycle and migratory abnormalities, resulting in a thinner cortical plate (20–23).

Underlying its complex biological functions, Pax6 protein has three distinct domains, the PD, the HD, and the transactivation domain. The PD contains two helix-turn-helix motifs,

* This work was supported, in whole or in part, by National Institutes of Health Grants EY017061 and EY018868 (to X. Z.).
[1] To whom correspondence should be addressed. Tel.: 317-274-1062; E-mail: xz4@iu.edu.
[2] The abbreviations used are: Pax, paired box; PD, paired domain; HD, homeodomain; SVZ, subventricular zone; R, reverse; F, forward; pHH3, phosphorylated histone H3; E, embryonic day.

referred to as the "PAI" and the "RED" motif regions, respectively, that are necessary for DNA recognition and binding (24). The PD may also cooperate with the DNA-binding HD to promote transcription via the transactivation domain, a proline-, serine-, threonine-rich linker domain at the C terminus (25). Pax6(5a), an alternatively spliced isoform of Pax6, contains a 14-amino acid insert within the PD that considerably changes its DNA binding specificity: the canonical PD binds to DNA via its N-terminal PAI domain, whereas the Pax6(5a) PD targets DNA with the C-terminal RED domain (24). Although the *Pax6*(*5a*) isoform only constitutes up to 20% of total *Pax6* transcripts, loss of *Pax6*(*5a*) in human and mouse results in distinct ocular phenotypes (24, 26, 27). In addition, overexpression of *Pax6*(*5a*) in cerebral cortex progenitors was observed to inhibit cell proliferation without affecting cell fate, whereas overexpression of the canonical *Pax6* inhibited cell proliferation but also potently increased neurogenesis (26, 28). These results led to the conclusion that Pax(5a) only controls cell proliferation, whereas Pax6 canonical isoform regulates both cell growth and fate determination.

A homologous PD is also the defining feature of the larger *Pax* gene family, which otherwise harbors considerable sequence variations within its nine family members. Unlike Pax6, for example, Pax2 retains a partial one-helix HD and an eight-amino acid octapeptide motif, which is functionally important for transcriptional inhibition (for a review, see Ref. 29). Using a PCR-based seletion method, Epstein *et al.* (30) showed that the *Pax6* PD and *Pax2* PD share strikingly similar consensus binding sequences. Nevertheless, although ectopic expression of Pax6 can sometimes induce eye formation outside the ocular region, Pax2 is known for its distinct control of urogenital development. Only during early eye development when *Pax2* and *Pax6* are initially co-expressed in the optic vesicle do they play redundant roles in retinal pigmented epithelium specification (31, 32). But even in the eye, *Pax2* and *Pax6* expressions quickly diverge through mutual repression to control optic stalk and neural retina development, respectively (33). It remains unclear how these two transcriptional regulators that share an almost identical consensus PD binding sequence can have sometimes redundant but often divergent functions in embryogenesis.

In our present study, we sought to examine the functional specificity of the *Pax* genes in neural development by replacing the *Pax6* coding region with either *Pax2* or *Pax6*(*5a*) cDNA, which led to induction of *Pax2* and *Pax6*(*5a*) in the endogenous *Pax6* expression domains. Although neither ectopically expressed transcription factor could rescue eye development, the ventral patterning of the neural tube was partially restored by the *Pax6*(*5a*) and *Pax2* knock-in. In contrast to previous reports that *Pax6*(*5a*) only affects cell proliferation but not cell fate in the telencephalon, we showed that ectopic *Pax6*(*5a*) reversed both dorsoventral patterning and progenitor proliferation defects, although boundary formation was not recovered. Interestingly, ectopic *Pax2* achieved stronger rescue of *Pax6* telencephalon patterning and neurogenesis than *Pax6*(*5a*) despite the fact that *Pax2* diverges from *Pax6* and *Pax6*(*5a*) outside the PD domain. Using a *Pax6* direct downstream target, the proneural gene *Ngn2*, as an example, we showed that the extent of rescue closely correlated with the binding affinities of Pax2 and Pax6(5a) PDs on the known *Ngn2* enhancer. Therefore, whereas the entire Pax6 protein is necessary for eye development, the binding specificity of the PD is largely sufficient to determine the functional specificity of Pax2, Pax6, and Pax6(5a) in forebrain and neural tube development.

EXPERIMENTAL PROCEDURES

Pax6 Targeting Vector Construction—The *Pax6* targeting vector was generated using the recombineering method (34, 35). Briefly, a minitargeting vector containing a *Neo* selection cassette and a *Pax6*(*5a*) full-length cDNA (IMAGE clone number 4008490) was used to replace the *Pax6* genomic sequence from exons 4 to 13 contained in a 129S6/SvEvTac Bac clone (BACPAC Resources Center at Children's Hospital Oakland Research Institute, catalogue number RP22-55A14). Through homologous recombination, the translation start site of *Pax6*(*5a*) cDNA was fused exactly at the original ATG codon within *Pax6* exon 4. The excision of the *Neo* cassette by Cre recombinase left behind a *de novo* NcoI site and a single *loxP* site in front of the *Pax6*(*5a*) cDNA. Using the gap repair method, the *Pax6*(*5a*) cDNA and the flanked 4.2- and 6-kb *Pax6* genomic sequences were cloned into pAY253, a low copy number *MC1TK*-containing plasmid that can accommodate large DNA inserts. A second round of minitargeting then placed behind the *Pax6*(*5a*) cDNA another *Neo* cassette, a stop cassette (five copies of poly(A) sequence), a single *loxP* site, and a full-length cDNA for *Pax2* followed by a new BamHI site (Fig. 1*A*). The resulting *Pax6* targeting vector was verified by direct sequencing.

Generation of Mouse Lines—ES cells (129S6/SvEvTac) electroporated with the linearized *Pax6* targeting vector were screened for successful homologous recombination by Southern blot using both 5′ (NcoI) and 3′ (BamHI) external probes (Fig. 1*B*). The positive ES cells were used to generate $Pax6^{5a}$ chimeric mice by pronuclear injection into C57BL/6 mouse blastocysts. Tail biopsies were collected, and genotype PCR was performed to confirm the $Pax6^{5a}$ allele (primers: $Pax6^{5a}$ F, 5′-GATGCAAAAGTCCAGGTGCT-3′; $Pax6^{5a}$ R, 5′-TTCCCAAGCAAAGATGGAAG-3′) (Fig. 1*C*). The $Pax6^{5a/+}$ mice were crossed to the *Ella-Cre* mice (The Jackson Laboratory, stock number 003724) to remove the *Pax6*(*5a*) cDNA and the *Neo* and the stop cassettes in the germ line. The resulting $Pax6^{Pax2/+}$ mice were confirmed by genotype PCR (primers: $Pax6^{Pax2}$ F, 5′-AAAGTGGTGGACAAGATTGC-3′; $Pax6^{Pax2}$ R, 5′-TTAGGGACAGAGCCCTCAGA-3′). *Pax6* small eye mutant embryos ($Pax6^{Sey\text{-}Neu/Sey\text{-}Neu}$) were kindly provided by James Li (University of Connecticut Health Center, Farmington, CT) (10, 36).

The presence of a vaginal plug was considered 0.5 days postcoitum or E0.5. All experimental procedures involving mice were humanely performed in accordance with the Laboratory Animal Research Center at Indiana University.

Immunohistochemistry and Histology—Fluorescent immunohistochemistry of cryosections and paraffin sections were performed as described previously (37–39). The following antibodies were used: mouse anti-Islet1 (1:10), anti-Pax6 (1:10), and anti-Nkx2.2 (1:10) (all from Developmental Studies

Hybridoma Bank, Iowa City, IA); mouse anti-Mitf (1:50) (Thermo Scientific, Fremont, CA); rabbit anti-Sox2 (1:800) (Chemicon International, Billerica, MA); rabbit anti-Pax2 (1:100) and rabbit anti-Pax6 (1:250) (both from Covance, Berkeley, CA); rabbit anti-phosphohistone H3 (Ser-10) (1:500) (Upstate, Temecula, CA); and rabbit anti-Ptf1a (1:100) (kindly provided by Dr. Jane E. Johnson, University of Texas Southwestern Medical Center, Dallas, TX). Secondary antibodies for all experiments were either Alexa Fluor 488- (1:250) or Alexa Fluor 555 (1:500)-conjugated anti-mouse and anti-rabbit IgG (Jackson ImmunoResearch Laboratories, West Grove, PA). For histology of E14.5 paraffin sections of cerebral cortex, hematoxylin and eosin staining was performed as described previously (37).

RNA in Situ Hybridization—RNA *in situ* hybridization experiments for whole-mount embryos and slide sections were performed as described previously (37–39). Antisense probes were generated from cDNAs for *Crx* (from Valerie Wallace, Ottawa Health Research Institute, Ottawa, Ontario, Canada), *Foxe3* (from Dr. Milan Jamrich, Baylor College of Medicine, Houston, TX), *Pax2* and *Pax6* (both generously provided by Richard Maas, Brigham and Women's Hospital, Harvard Medical School, Boston, MA), *Ngn2* (kindly provided by Lin Gan, University of Rochester, Rochester, NY), *Mash1* (kindly provided by Alexandra Joyner, Memorial Sloan-Kettering Cancer Center New York, NY), *Math5* (from Dr. Tom Glaser, University of California, Davis, CA), and *Sfrp2* (a generous gift from Andrew McMahon, Harvard University, Boston, MA).

Quantitative Real Time RT-PCR—To compare the expression levels of knock-in *Pax6*(*5a*) and *Pax2* in embryonic brain at E14.5, they were individually correlated with the endogenous *Pax6* expression level in $Pax6^{5a/+}$ and $Pax6^{Pax2/+}$ mutants by quantitative real time RT-PCR as described previously (34). PCR primers used were as follows: *Pax6*(*5a*)/*Pax6*: F, GCGCAGACGGCATGTATGATA; R, GGGTTGCCCTGGTACTGAAG; *Pax2*: F, AAGCCCGGAGTGATTGGTG; R, CAGGCGAACATAGTCGGGTT (acquired from Harvard PrimerBank). To determine any differences in expression levels of *Pax6* and *Pax6*(*5a*), the combined expression levels of *Pax6* and *Pax6*(*5a*) were compared in wild type and $Pax6^{5a/+}$ embryos. In another experiment, *Pax2* knock-in and *Pax6* expression levels were compared within $Pax6^{Pax2/+}$ mutants. The knock-in *Pax2* expression levels were calculated by subtracting endogenous *Pax2* levels in wild type littermates. To determine the absolute transcript levels, plasmids encoding *Pax6* and *Pax2* cDNA were used to calibrate Ct values. *Gapdh* was used as an endogenous control to normalize the Ct values. Three embryos were used for each genotype, and all experiments were run in triplicates. The statistical significance was calculated by Student's *t* test.

Data Analysis—Quantification of cortical plate and phosphorylated histone H3-positive ($pHH3^+$) cells was performed as described previously (26). Briefly, the quantification of cortical plate was determined in hematoxylin- and eosin-stained E14.5 cerebral cortex sections throughout rostral, intermediate, and caudal levels (40, 41). The length of a line, measured by the ImageJ program, from the ventricular surface to the pial surface served as the total cortical thickness. The length of a second line drawn from the apical and basal side of the cortical plate served as the thickness of the cortical plate. The relative width of the cortical plate was expressed as the proportion of the overall thickness of the cerebral cortex. Quantification of $pHH3^+$ cells at subventricular zone (SVZ) cells was performed by placing a 150-μm-wide square covering the entire cortical thickness parallel to the ventricular surface and counting all $pHH3^+$ cells five or more cell diameters away from the ventricular surface (26). Quantification of the Nkx2.2-positive domain in the developing neural tube was performed by counting the number of cell rows in the neural tube positive for Nkx2.2 immunofluorescence and expressing it as the proportion of the total number of neural tube cell rows in each E10.5 C1-R7 level section (17). The statistical significance was calculated by one-way analysis of variance and Tukey's post hoc tests.

Paired Domain-Glutathione S-Transferase Fusion Protein Preparations—The pGEX-Pax6 and pGEX-Pax6(5a) GST-paired domain expression plasmids were generously provided by Richard Maas (Brigham and Women's Hospital, Harvard Medical School, Boston MA) (24, 30). For pGEX-Pax2 GST, a full-length cDNA clone for murine *Pax2*, pPax2-CMV (also kindly provided by Richard Maas, Brigham and Women's Hospital, Harvard Medical School, Boston MA) was used as a template in a PCR with primers (F, 5′-CTCGGATCCATGGATATGCACTGCAAAGCAGACC-3′; R, 5′-ATCGAATTCGAACTTTGGTCCGGATGATCCTGTT-3′) to amplify the sequence corresponding to amino acids 1–128 for Pax2. This PCR product was then cloned into the BamHI and EcoRI sites of pGEX4T1, and the resulting clone was verified by direct sequencing. Large scale purification of GST fusion proteins was performed in BL21 *Escherichia coli*.

Electrophoretic Mobility Shift Assay (EMSA)—EMSA reactions were carried out as described previously (42, 43). The following oligonucleotide probes were used: P6CON, 5′-GATCAGGAAAAATTTTCACGCTTGAGTTCACAG-3′ (24); 5aCON, 5′-GATCCAATGTTCATTGACTCTCGAG-3′ (24); E1.1, 5′-TCATTCACGCCTAGAAGCAG-3′ (44); mtE.1, 5′-TCACTAGTAACGAGAAGCAG-3′ (44); E1.5a, 5′-ATCTCAATCAACAATCCATTAGAACTCA-3′; and mtE1.5a, 5′-TCACTAGTAACGCCATTAGAACTCA. These oligonucleotides were end-radiolabeled by T4 kinase with [γ-^{32}P]ATP prior to annealing oligonucleotides of complimentary sequence.

RESULTS

Generation of $Pax6^{5a}$ and $Pax6^{Pax2}$ Alleles—To investigate the functional specificity of *Pax6*, we took a cDNA knock-in approach to determine whether *Pax6* can be functionally replaced by either *Pax2*, which shares a similar DNA-binding PD, or *Pax6*(*5a*), which shares the same homeodomain and the transactivation domain. The $Pax6^{5a/+}$ allele was generated by fusing a *Pax6*(*5a*) cDNA in-frame to the original *Pax6* start codon, whereas the $Pax6^{Pax2/+}$ allele was subsequently derived by Cre-mediated excision of the *Pax6*(*5a*) and a stop cassette from the $Pax6^{5a/+}$ allele, allowing the remaining *Pax2* cDNA to be expressed (Fig. 1, *A–C*). In homozygous mutants, *Pax6*(*5a*) and *Pax2* RNAs were expressed in the endogenous *Pax6* spatiotemporal pattern in the eye, telencephalon, and neural tube, whereas in heterozygous eyes ($Pax6^{Pax2/+}$), ectopic *Pax2* expression arose at the expense of the endogenous *Pax6* tran-

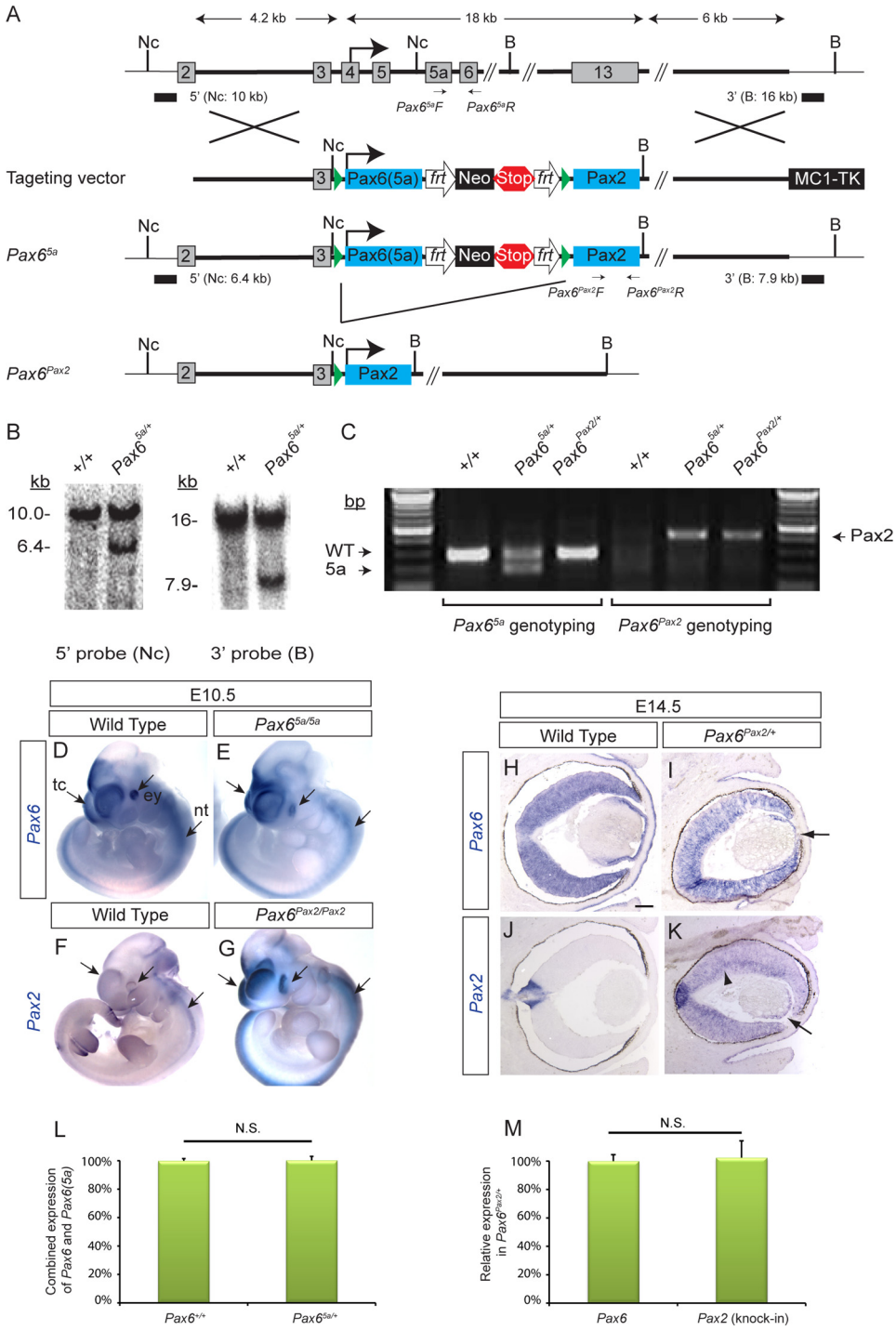

FIGURE 1. **Cloning strategy for *Pax6*^{5a} and *Pax6*^{Pax2} knock-ins.** *A*, the coding region of *Pax6* (exons 4–13) was replaced by a cDNA for *Pax6*(*5a*) followed by a neomycin (*Neo*) cassette, a stop cassette (five copies of poly(A) sequence), and a cDNA for *Pax2*. *Frt* and *LoxP* sites are represented by *open arrows* and *solid triangles*, respectively. *Nc*, NcoI; *B*, BamHI. *B*, for Southern blot confirmation, genomic DNA extracted from targeted ES cells digested with either NcoI or BamHI was hybridized with the 5′ or the 3′ external probes, respectively. Predicted fragment sizes were obtained for the correctly targeted clones. *C*, genotyping for *Pax6*^{5a} and *Pax6*^{Pax2} alleles. *D–G*, using a *Pax6* 3′-UTR probe (common to both *Pax6* and *Pax6*(*5a*)) and a *Pax2* probe, we showed that *Pax6*(*5a*) and *Pax2* RNAs were expressed ectopically within the endogenous *Pax6* expression domains at embryonic day 10.5 (*arrows*). *tc*, telecephalon; *ey*, eye; *nt*, neural tube. *H–K*, in *Pax6*$^{Pax2/+}$ eyes, there was a decrease in *Pax6* transcripts but a corresponding expansion of *Pax2* expression from the optic disc to the whole retina (*arrowhead*) and the lens (*arrow*). *L*, quantitative real time PCR was performed on E14.5 brain tissues with primers that recognize the domain shared by *Pax6* and *Pax6*(*5a*). After normalization using *Gapdh* expression, the combined expression of *Pax6* and *Pax6*(*5a*) was shown to be the same in *Pax6*$^{+/+}$ and *Pax6*$^{5a/+}$ embryos, demonstrating that *Pax6*(*5a*) was transcribed as efficiently as endogenous *Pax6*. *M*, the numbers of *Pax6* and *Pax2* transcripts in *Pax6*$^{Pax2/+}$ embryos were determined by quantitative real time PCR using standard curves generated with *Pax6* and *Pax2* cDNA plasmids and normalized using *Gapdh* expression. After subtracting endogenous expression of *Pax2* determined from wild type samples, the expression level of *Pax2* knock-in allele was found to be the same as that for endogenous *Pax6* in *Pax6*$^{Pax2/+}$ embryos. $n = 3$ for each genotype. *N.S.*, not significant. *Scale bar*, 100 μm. *Error bars* represent S.E.

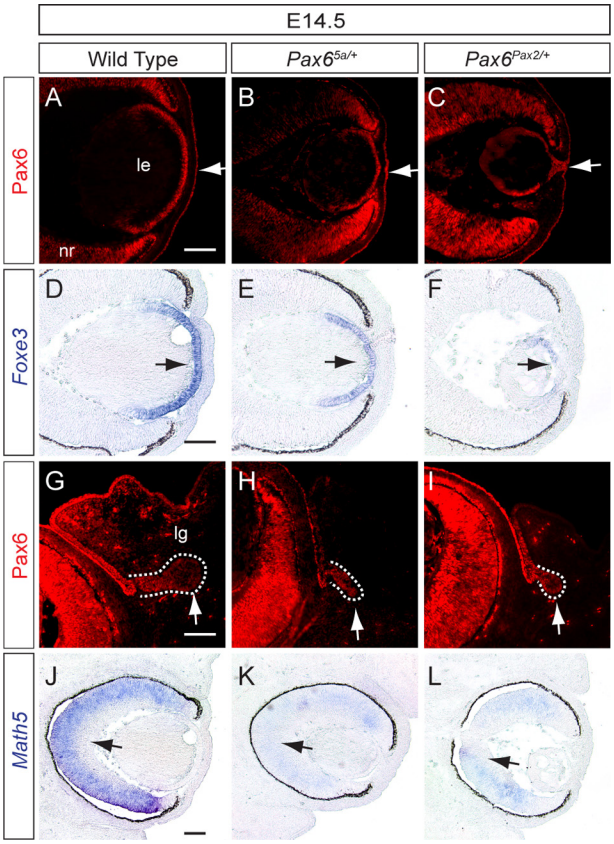

FIGURE 2. **Partial rescue of *Pax6* heterozygous lens phenotype by *Pax6*(*5a*) but not by *Pax2*.** *A–C*, persistent corneal-lenticular stalk (*arrow* in *C*) was present only in E14.5 $Pax6^{Pax2/+}$ mutants but not in wild type and $Pax6^{5a/+}$ eyes. *D–F*, *Foxe3* expression (*arrows*) was reduced more significantly in $Pax6^{Pax2/+}$ mutants than in $Pax6^{5a/+}$ eyes. *G–L*, both $Pax6^{Pax2/+}$ and $Pax6^{5a/+}$ mutants displayed smaller lacrimal gland buds (outlined in *white dashed lines*) and reduced expression of retinal differentiation gene *Math5* (*arrows*). *Scale bar*, 100 μm.

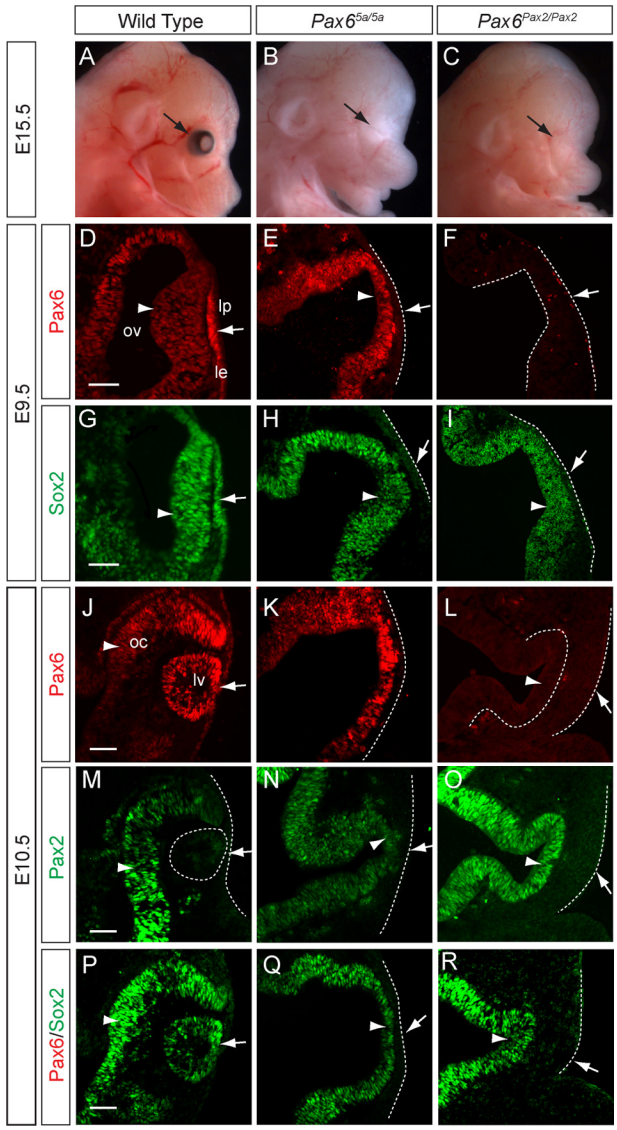

FIGURE 3. **Lens induction failure in $Pax6^{5a/5a}$ and $Pax6^{Pax2/Pax2}$ knock-in mutants.** *A–C*, no obvious eye structure was observed in the E15.5 $Pax6^{5a/5a}$ and $Pax6^{Pax2/Pax2}$ mutants (*arrows*). *D–F*, using an antibody that recognized both Pax6 and Pax6(5a) protein, we detected Pax6 in the wild type lens placode (thickening of lens surface ectoderm) but not Pax6(5a) in the $Pax6^{5a/5a}$ mutant surface ectoderm (compare *D* and *E*, *arrows*). No lens placode was formed in either E9.5 $Pax6^{5a/5a}$ or $Pax6^{Pax2/Pax2}$ mutants. *ov*, optic vesicle; *lp*, lens placode; *le*, lens ectoderm. *G–I*, *Sox2* expression was absent from lens surface ectoderm (*arrows*) but present in developing optic vesicles of both knock-in mutants at E9.5 (*arrowheads*). *J–R*, in both knock-in mutants at E10.5, lens vesicle and optic cup failed to form, and Pax6, Pax6(5a), Pax2, and Sox2 expressions were absent from lens surface ectoderm (*arrows*). *lv*, lens vesicle; *oc*, optic cup. *Scale bar*, 50 μm.

scripts (Fig. 1, *D–K*). By quantitative real time PCR, we confirmed that *Pax6*(*5a*) and *Pax2* were both expressed at a level similar to that of the endogenous *Pax6* in $Pax6^{5a/+}$ and $Pax6^{Pax2/+}$ embryos, respectively (Fig. 1, *L* and *M*). Furthermore, no read-through transcription or translation of *Pax2* was detected in $Pax6^{5a/5a}$ mutants (see Figs. 5, *C* and *G*, and 6*C*). These results supported the correct gene targeting and preservation of major transcriptional regulatory elements in the $Pax6^{5a}$ and $Pax6^{Pax2}$ alleles.

Pax6(5a), but Not Pax2, Prevents Persistent Lens Stalk in Heterozygous Animals—We first examined $Pax6^{5a/+}$ and $Pax6^{Pax2/+}$ embryos to determine whether they resembled *Pax6* heterozygous nulls. At E14.5, Pax6 staining revealed clear separations between lens and cornea in both wild type and $Pax6^{5a/+}$ embryos (Fig. 2, *A* and *B*, *arrows*). In $Pax6^{Pax2/+}$ embryos, however, there still existed a persistent corneal-lenticular stalk (Fig. 2*C*, *arrow*), a known ocular defect in $Pax6^{Seu/+}$ mutants. Consistent with this, *Pax6* downstream gene *Foxe3* was only modestly reduced in $Pax6^{5a/+}$ embryos but was nearly absent in $Pax6^{Pax2/+}$ lens (Fig. 2, *D–F*, *arrows*) (45). In contrast, the budding of lacrimal gland and retinal expression of *Math5*, two features also known to be sensitive to *Pax6* gene dosage, were both disrupted in $Pax6^{5a/+}$ and $Pax6^{Pax2/+}$ embryos (Fig. 2, *G–L*, *arrows*) (34, 46, 47). Therefore, *Pax6*(*5a*), but not *Pax2*, partially substituted for *Pax6* function in lens development.

Failure of Lens Induction in the $Pax6^{5a/5a}$ and $Pax6^{Pax2/Pax2}$ Embryos—The $Pax6^{5a/5a}$ and $Pax6^{Pax2/Pax2}$ embryos were recovered at the expected Mendelian ratio at E15.5, but they lacked any obvious eye structures (Fig. 3, *A–C*, *arrows*). This prompted us to examine lens induction, the pivotal morphogenetic event in early eye development. The murine embryonic eye develops in response to signaling interactions between two Pax6-expressing embryonic tissues, the head surface ectoderm and optic vesicle. After coming in physical contact with the

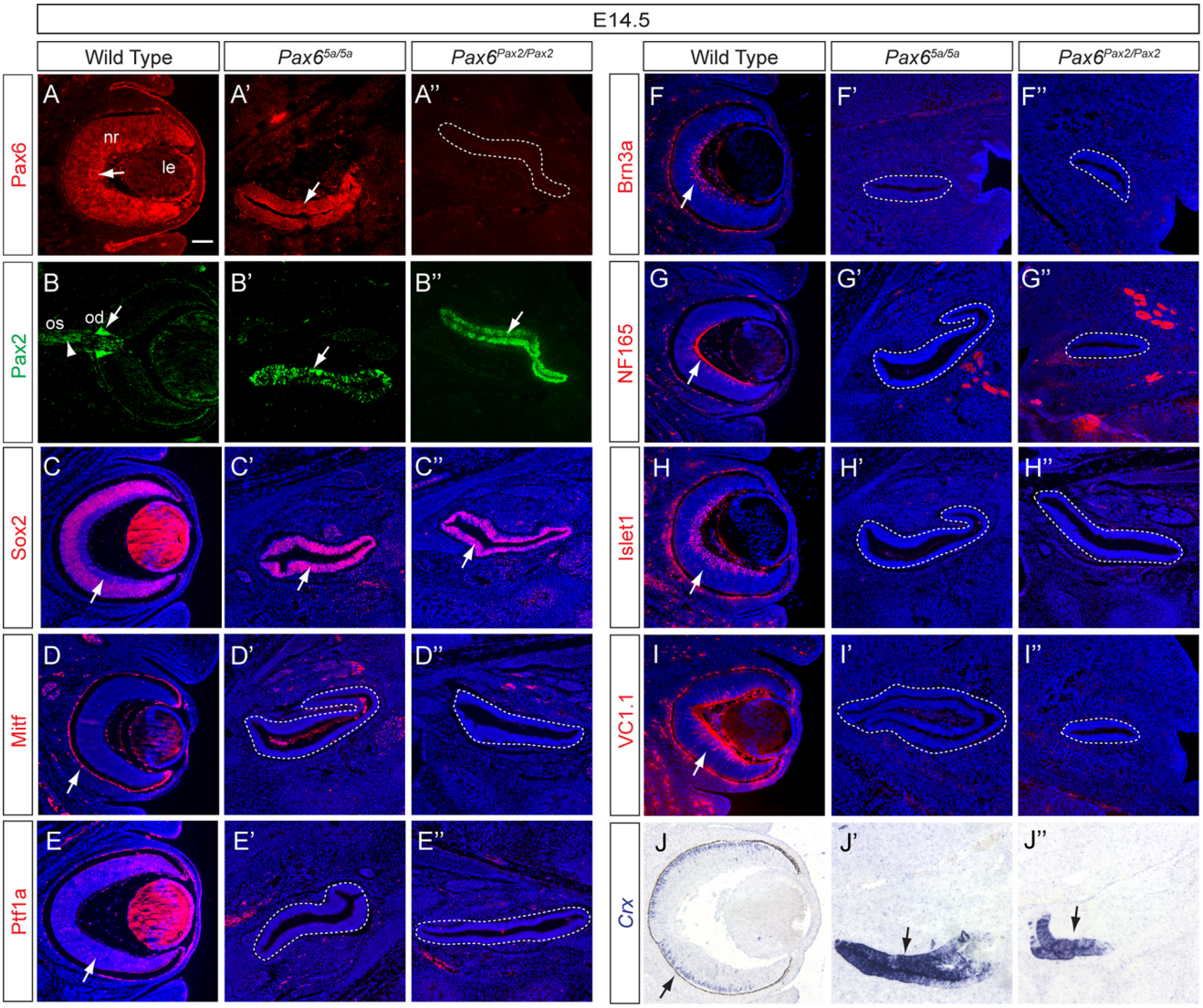

FIGURE 4. **Defective retinal development in *Pax6*$^{5a/5a}$ and *Pax6*$^{Pax2/Pax2}$ mutants.** *A–B″*, Pax6(5a) and Pax2 were expressed in the residual *Pax6*$^{5a/5a}$ and *Pax6*$^{Pax2/Pax\ 2}$optic vesicles (*arrowhead*). *nr*, neural retina; *le*, lens; *os*, optic stalk; *od*, optic disc. *C–D″*, entire mutant optic vesicles (*dashed lines*) expressed neural retinal marker Sox2 but not retinal pigmented epithelium marker Mitf. *E–J″*, the retinal differentiation factors Ptf1a, Brn3a, NF165, Islet1, and VC1.1 were lost in the mutant optic vesicles (*dashed lines*), but photoreceptor cell differentiation gene *Crx* was ectopically expressed (*arrows*). *Scale bar*, 100 μm.

optic vesicle at E9.5, the wild type surface ectoderm thickened to form the presumptive lens placode where Pax6 up-regulated its own expression (Fig. 3*D*, *arrow*). In contrast, no Pax6-positive lens placode was observed in the *Pax6*$^{5a/5a}$ and *Pax6*$^{Pax2/Pax2}$ mutants, indicating a failure of the *Pax6* autoregulatory loop (Fig. 3, *E–F*, *arrows*). As a consequence, the expression of Sox2, a *Pax6* downstream transcription factor in lens placode development, was also extinguished (Fig. 3, *G–I*, *arrows*). At E10.5 when the wild type lens placode invaginated to form a lens vesicle, the *Pax6*$^{5a/5a}$ and *Pax6*$^{Pax2/Pax2}$ mutants failed to form any lens structures, and Pax6, Pax2, and Sox2 were completely absent on the remaining surface ectoderm (Fig. 3, *J–R*, *arrows*). It is important to note that *Pax2* expression was still detected in *Pax6*$^{Pax2/+}$ lens (Fig. 1*K*, *arrow*), indicating that our knock-in alleles did not lose any essential lens enhancer. Taken together, these results demonstrated that *Pax6*(*5a*) and *Pax2* were unable to activate the *Pax6* autoregulatory mechanism in the presumptive lens placode, which led to the loss of lens development.

Retinal Development Is Disrupted in the Pax6$^{5a/5a}$ *and Pax6*$^{Pax2/Pax2}$ *Mutants*—Previous studies have shown that retinal differentiation was initially accelerated in the *Pax6*-null mutants, but the neurogenesis was eventually aborted (15, 16). Thus, we examined whether retinogenesis still occurred in the *Pax6*$^{5a/5a}$ and *Pax6*$^{Pax2/Pax2}$ mutants. In the E14.5 wild type embryos, Pax6 was detectable throughout the neural retina, whereas Pax2 was restricted to the optic stalk and the optic disc (Fig. 4, *A* and *B*, *arrow* and *arrowhead*). In contrast, the *Pax6*$^{5a/5a}$ optic vesicle expressed both Pax6(5a) and Pax2 (Fig. 4, *A′* and *B′*), whereas the *Pax6*$^{Pax2/Pax2}$ optic vesicle only expressed Pax2 (Fig. 4, *A″* and *B″*). Furthermore, both mutant optic vesicles were positive for Sox2, here a retinal progenitor marker, but negative for Mitf, a retinal pigmented epithelium marker (Fig. 4, *C–D″*). These results indicated that the patterning of optic vesicle into retinal pigmented epithelium, optic disc, and neural retina was abolished in the *Pax6*$^{5a/5a}$ and *Pax6*$^{Pax2/Pax2}$ mutants. We also provide evidence that neurogenesis was disrupted in the mutants. Ptf1a is a transcription

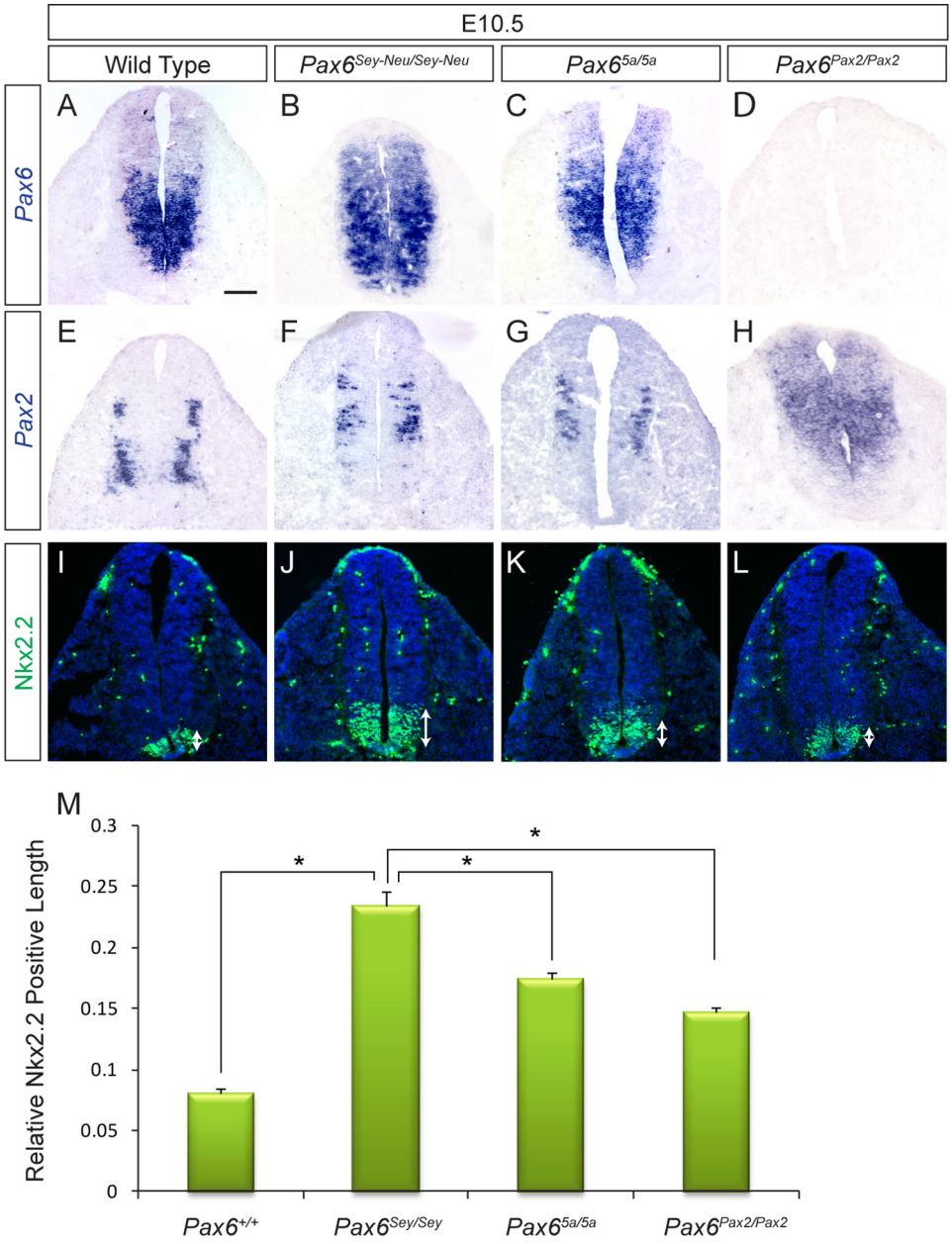

FIGURE 5. **Correction of Nkx2.2 expression by Pax2 and Pax6(5a) in neural tube.** *A–H*, *Pax6*(*5a*) and *Pax2* were expressed within the endogenous *Pax6* neural tube domain in the E10.5 $Pax6^{5a/5a}$ and $Pax6^{Pax2/Pax2}$ mutants, respectively. *I–L*, the suppression of Nkx2.2 by Pax6 was disrupted in the Pax6-null ($Pax6^{Sey\text{-}Neu/Sey\text{-}Neu}$) mutants, allowing for Nkx2.2 expression to expand dorsally (*arrows*). A significant decrease in Nkx2.2 expansion was observed in the $Pax6^{5a/5a}$ and $Pax6^{Pax2/Pax2}$ mutants. *M*, measurement of the relative length of Nkx2.2-positive neural tube (*, $p < 0.05$; $n = 3$). *Scale bar*, 100 μm. *Error bars* represent S.E.

factor important for retinal amacrine and horizontal cells. Its expression was completely lost in the $Pax6^{5a/5a}$ and $Pax6^{Pax2/Pax2}$ mutant optic vesicles (Fig. 4, *E–E″*). Brn3a and NF165, markers for newly differentiated ganglion cells, were similarly abrogated (Fig. 4, *F–G″*). Islet1, which marks differentiating retinal ganglion and amacrine cells, was also absent in the mutants (Fig. 4, *H–H″*). It has been shown previously that the *Pax6*-null retina still expresses the photoreceptor determination gene *Crx* and amacrine cell differentiation marker VC1.1 (15). Interestingly, we did not detect any VC1.1 expression in our mutants, but *Crx* expression was indeed expanded to most of the residual optic vesicles (Fig. 4, *I–J″*, *arrows*). Taken together, these ocular defects demonstrate the strict requirement of canonical *Pax6* for lens and retinal development.

Pax6(5a) and Pax2 Partially Substitute for Pax6 in Suppressing Ectopic Nkx2.2 Expansion in the Neural Tube—Considering that *Pax6* is required for patterning the ventral neural tube, we next asked whether *Pax6*(*5a*) or *Pax2* could recapitulate the role of *Pax6* as a repressor of homeodomain transcription factor Nkx2.2 expression (17, 48). By E10.5, wild type *Pax6* expression was detected in the ventral neural tube, whereas *Pax2* was expressed in the neural tube bilaterally flanking the dorsoventral midline (Fig. 5, *A* and *E*). This was in contrast to the ectopic expression of *Pax6*(*5a*) and *Pax2* within the neural tube-*Pax6*

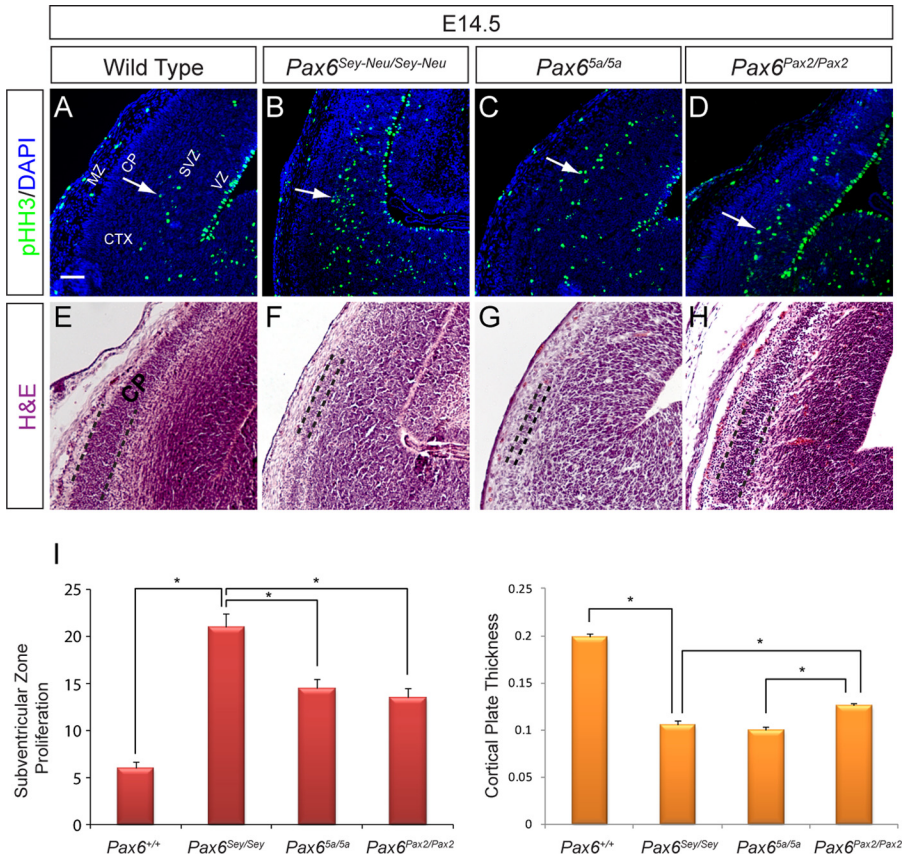

FIGURE 6. ***Pax2* and *Pax6*(*5a*) partially rescued cell proliferation defects in telencephalon.** *A–D*, an increase in cortical progenitor cell proliferation as indicated by pHH3 staining was evident in the SVZ (*arrow*) of the *Pax6*$^{Sey\text{-}Neu/Sey\text{-}Neu}$ mutants (*B*). A statistically significant decrease in SVZ cell proliferation was observed in both knock-in mutants. *E–H*, hematoxylin and eosin staining of E14.5 telencephalon showed a partial rescue of cortical plate (*CP*) thickness in the *Pax6*$^{Pax2/Pax2}$ telencephalon. *I*, measurements of SVZ proliferation and cortical plate thickness (*, $p < 0.05$; $n = 3$). *VZ*, ventricular zone; *CTX*, cortex; *MZ*, marginal zone. *Scale bar*, 100 μm. *Error bars* represent S.E.

expression domains in the corresponding knock-in mutants (Fig. 5, *C*, *D*, and *F–H*). As expected, Nkx2.2 expression expanded dorsally in the *Pax6*-null (*Pax6*$^{Sey\text{-}Neu/Sey\text{-}Neu}$) mutants, confirming the antagonistic interaction between Pax6 and Nkx2.2 (Fig. 5, *I* and *J*, *arrows*). In both *Pax6*$^{5a/5a}$ and *Pax6*$^{Pax2/Pax2}$ mutants, however, the dorsal expansion of Nkx2.2 appeared to be partially reduced compared with the *Pax6*-null mutants (Fig. 5, *K* and *L*, *arrows*). By calculating the proportion of Nkx2.2-positive cells per total number of neural tube cells, we confirmed that the suppression of ectopic Nkx2.2 expression was statistically significant for *Pax6*$^{5a/5a}$ and *Pax6*$^{Pax2/Pax2}$ mutants (Fig. 5*M*).

Partial Rescue of Telencephalic Cell Proliferation and Neurogenesis by Pax2—Transgenic overexpression studies suggest that *Pax6* and *Pax6*(*5a*) both have antiproliferative roles in the embryonic cortex (26, 28). To assess any changes in cortex cell proliferation in our mutants, mitotic cells in E14.5 coronal cortex sections were immunolabeled with anti-pHH3. Consistent with previous studies, E14.5 *Pax6*$^{Sey\text{-}Neu/Sey\text{-}Neu}$ mutants exhibited a significant increase in cell proliferation within the SVZ compared with the wild type cortex, whereas the ventricular zone mitotic index remained the same (Fig. 6, *A* and *B*, *arrows*) (26). However, there was a statistically significant reduction in the number of pHH3-positive subventricular zone cells in both *Pax6*$^{5a/5a}$ and *Pax6*$^{Pax2/Pax2}$ mutants compared with the *Pax6*-null mutants (*Pax6*$^{Sey\text{-}Neu/Sey\text{-}Neu}$), indicating a partial rescue of telencephalic progenitor cell inhibition (Fig. 6, *C*, *D*, and *I*). After terminal cell division, newborn neurons migrate to beneath the pial surface to form a conspicuous band called the cortical plate (Fig. 6, *E–H*, telencephalic area flanked by *dotted lines*). Relative to the total cortical thickness in the lateral cortex, the cortical plates in the *Pax6*$^{Sey\text{-}Neu/Sey\text{-}Neu}$ and the *Pax6*$^{5a/5a}$ mutants were both thinner than that of the wild type embryos. The *Pax6*$^{Pax2/Pax2}$ mutants, however, exhibited a significant increase in cortical thickness, suggesting that, unlike *Pax*(*5a*), *Pax2* could partially rescue neurogenesis in the *Pax6*-deficient cortex (Fig. 6*I*).

Stronger Rescue of Telencephalon Patterning in Pax6$^{Pax2/Pax2}$ *Mutants than in Pax6*$^{5a/5a}$ *Mutants*—Given the vital role of *Pax6* in the dorsoventral specification of telencephalic progenitors, we next examined the expression patterns of three well characterized *Pax6* downstream targets within the developing telencephalon at E14, namely *Ngn2*, *Mash1*, and *Sfrp2*. Pax6 expression was normally confined to the dorsal E14.5 telencephalon in the wild type embryos as was the expression of Pax6(5a) and Pax2 in the *Pax6*$^{5a/5a}$ and the *Pax6*$^{Pax2/Pax2}$ mutants, respectively (Fig. 7, *A–D*, *arrows*). Consistent with previous reports, we observed in the *Pax6*$^{Sey\text{-}Neu/Sey\text{-}Neu}$ mutants a complete abrogation of telencephalic *Ngn2* expression in addition to an expanded expression of the ventral telencephalon-specific transcription factor *Mash1* into the dorsal telencephalon (Fig. 7, *F* and *J*, *arrows*) (26). In the *Pax6*$^{5a/5a}$

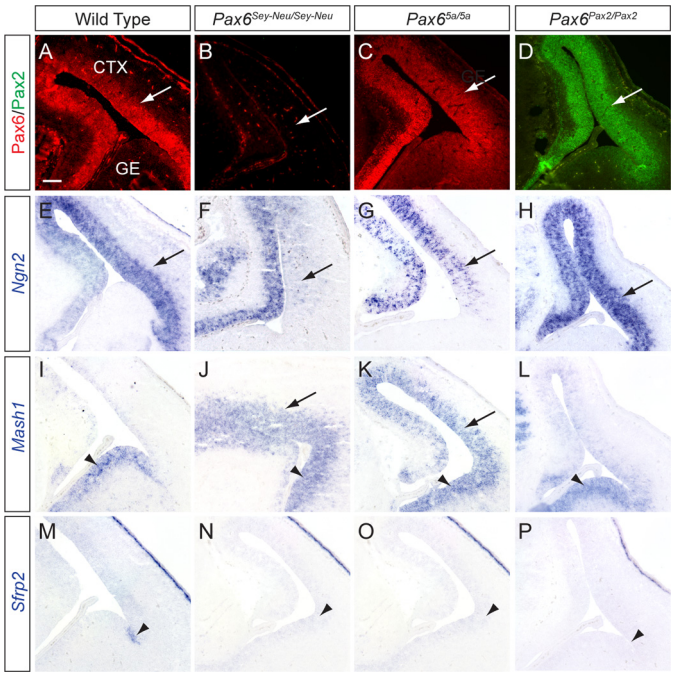

FIGURE 7. **Differential rescue of dorsoventral patterning in *Pax6*$^{5a/5a}$ and *Pax6*$^{Pax2/Pax2}$ mutant telencephalon.** *A–D*, Pax2 and Pax6 immunohistochemistry confirmed endogenous and ectopic protein expression within the dorsal telencephalon at E15.5 (*arrows*). *E–H*, *Pax6*-proneural gene target *Ngn2* RNA expression was lost in the *Pax6*$^{Sey\text{-}Neu/Sey\text{-}Neu}$ mutant dorsal telencephalon but partially recovered in the *Pax6*$^{5a/5a}$ mutant and fully rescued in the *Pax6*$^{Pax2/Pax2}$ mutant (*arrows*). *I–L*, *Pax6*$^{Sey\text{-}Neu/Sey\text{-}Neu}$ and *Pax6*$^{5a/5a}$ mutants showed misexpression of proneural gene *Mash1* in the dorsal telencephalon (*arrows*), whereas *Pax6*$^{Pax2/Pax2}$ displayed normal *Mash1* expression in ventral telencephalon (*arrowheads*). *M–P*, Wnt inhibitor *Sfrp2*, normally expressed at telencephalon dorsal-ventral boundary (*arrowheads*), was not detected in any of the mutants. All sections were coronal. *Scale bar*, 100 μm.

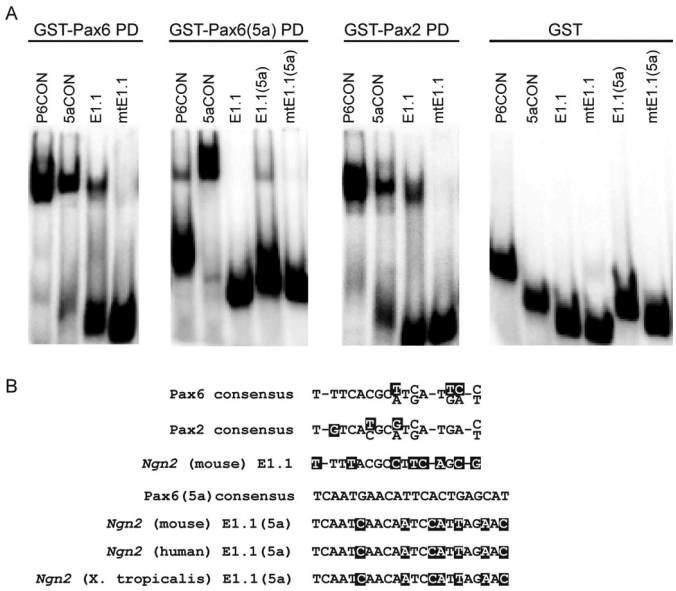

FIGURE 8. **Pax6(5a) and Pax2 paired domains bound the *Ngn2* telencephalic enhancer.** *A*, electrophoretic mobility shift assays performed with the recombinant Pax6, Pax6(5a), and Pax2 PD-GST fusion proteins. Pax6 and Pax2 paired domains bound the Pax6 and Pax6(5a) consensus binding sites (P6CON and 5aCON) and with a weaker affinity the *Ngn2* E1.1 enhancer element. Pax6(5a) paired domain preferentially bound 5aCON and the *Ngn2* E1.1(5a) site. The Pax6(5a)-E1.1(5a) binding was weaker than that of Pax2-E1.1. No binding complexes were observed with GST and the individual oligonucleotide probes. *B*, Pax2 and Pax6 paired domain consensus binding sites as well as the corresponding *Ngn2* enhancer E1.1 target sequence. The Pax6(5a) consensus binding site and its phylogenetically conserved binding sequence within the *Ngn2* E1.1 enhancer are shown.

mutants, however, there was a modest recovery of *Ngn2* expression in the dorsal telencephalon, but *Mash1* was still ectopically expressed (Fig. 7, *G* and *K*, *arrows*). Remarkably, *Mash1* expression in the *Pax6*$^{Pax2/Pax2}$ mutant was correctly confined to the ventral telencephalon despite the lack of endogenous *Pax6* expression, whereas *Ngn2* was strongly expressed in the dorsal telencephalon (Fig. 7, *H* and *L*, *arrow* and *arrowhead*). Of note, *Sfrp2*, a boundary marker between the dorsal cortex and ventral ganglionic eminence, was still absent in the *Pax6*$^{5a/5a}$ and *Pax6*$^{Pax2/Pax2}$ mutants, suggesting an incomplete rescue of telencephalic patterning (Fig. 7, *M–P*, *arrowheads*). Nevertheless, it is clear that *Pax2* and to a lesser extent *Pax6*(*5a*) can at least substitute for some of the canonical *Pax6* functions in the regionalization of the forebrain telencephalon.

Differential Binding of Pax6(5a) and Pax2 Paired Domains on Ngn2 E1 Enhancer—To understand the mechanism of differential rescue in the *Pax6*$^{5a/5a}$ and *Pax6*$^{Pax2/Pax2}$ mutants, we next investigated the regulation of *Ngn2*, one of the best characterized *Pax6* downstream targets in neural development. Previous studies have shown that the canonical Pax6 isoform through its PD binds to a low affinity site on the *Ngn2* E1 enhancer, which promotes *Ngn2* expression only in the telencephalic domains of high *Pax6* expression (44). To assess whether there could exist a direct physical interaction between the *Ngn2* E1 enhancer and Pax6(5a) or Pax2 PD, we performed DNA EMSAs using oligonucleotide probes containing sequences corresponding to the *Pax6* binding sites. As expected, the P6CON and 5aCON control probes, which contained previously identified consensus binding site sequences, strongly bound GST-Pax6-PD and GST-Pax6(5a)-PD respectively (Fig. 8*A*) (24, 30). In addition, we confirmed the previous finding that GST-Pax6-PD weakly bound the *Ngn2* E1 enhancer element probe E1.1 but not the mutated E1 enhancer probe mtE1.1 (Fig. 8*A*) (44). Although GST-Pax6-PD could also recognize the 5aCON control probe, GST-Pax6(5a)-PD was unable to bind the P6CON site effectively (Fig. 8*A* and data not shown). Consistent with this, we did not observe any binding between GST-Pax6(5a)-PD and the E1.1 element, confirming that the E1.1 sequence was indeed a canonical Pax6 PD binding site. Nevertheless, in the same *Ngn2* E1 enhancer, we identified a putative Pax6(5a)-specific binding sequence, named E1.1(5a), that is evolutionally conserved from human to frog (*Xenopus tropicalis*) (Fig. 8*B*). By EMSA, we observed that GST-Pax6(5a)-PD could bind to probe E1.1(5a) but not to the mutated negative control probe mtE1.1(5a), although the overall binding was weaker than that of GST-Pax6-PD on probe E1.1 (Fig. 8*A*). This suggested that Pax6(5a) could potentially utilize the E1.1(5a) site, but the interaction was likely weaker than that of canonical Pax6 on the *Ngn2* E1 enhancer. Finally, we showed that the GST-Pax2-PD bound to P6CON and 5aCON sequences with affinities similar to that of GST-Pax6-PD, whereas control GST protein failed to bind any of these probes, demonstrating that Pax6 and Pax2 PD indeed share the same DNA binding specificity (Fig. 8*A*). Importantly, the binding of GST-Pax2-PD on E1.1 was also significantly stronger than that of GST-Pax6(5a)-PD on E1.1(5a). Taken

together, these results showed that Pax6 and Pax2 PDs formed a stronger binding complex on the *Ngn2* E1 enhancer than did Pax6(5a) PD, which correlated well with the differential level of *Ngn2* expression in the $Pax6^{5a/5a}$ and $Pax6^{Pax2/Pax2}$ mutant telencephalon.

DISCUSSION

In this study, we performed gene replacement experiments to rigorously test the functional specificity of *Pax6*, *Pax6*(*5a*), and *Pax2 in vivo*. In both the $Pax6^{5a/5a}$ and $Pax6^{Pax2/Pax2}$ mutants, lens development was abolished because lens induction never occurred. Further analysis showed that *Pax2* and *Pax6*(*5a*) failed to be expressed in the lens placode, demonstrating that the lens-specific enhancer activity in the *Pax6* locus required canonical *Pax6*. The known *Pax6* lens enhancer, also termed the ectoderm enhancer, contains binding sites for Meis/Prep, Sox2, Oct1, and Pax6 (34, 43, 49–51). Because the recombinant Pax2 PD bound as strongly as Pax6 PD on this lens enhancer in EMSA (data not shown), the lack of lens enhancer activity in the $Pax6^{Pax2/Pax2}$ mutants suggests that Pax2 may be unable to synergistically interact with the other cofactors on this enhancer. Another possibility was that the Pax6 HD was also required for its autoregulation in lens development, which was supported by the previous finding that mutations in the *Pax6* HD disrupted eye but not brain development (52). In support of this idea, we observed persistent lens stalk in $Pax6^{Pax2/+}$, but not in $Pax6^{5a/+}$, embryos, suggesting that *Pax6*(*5a*) could partially substitute for canonical *Pax6* in lens development. However, it should be noted that the *Pax6* lens enhancer remained inactive in the $Pax6^{5a/5a}$ mutants despite the intact HD in *Pax6*(*5a*). Therefore, it is likely that both the PD and HD of *Pax6* were necessary for its optimum function in lens induction.

In retinal development, *Pax2* and *Pax6* have been shown to cooperate initially in retinal pigmented epithelium specification, but later on, they play antagonistic roles in optic stalk and optic cup development, respectively (31–33). In the $Pax6^{Pax2/Pax2}$ mutants, however, the residual optic vesicle expressed the neural retina markers Sox2 and Crx but not the retinal pigmented epithelium marker Mitf. This suggested that, without *Pax6*, *Pax2* alone could not maintain retinal pigmented epithelium or optic stalk fate. On the other hand, although ectopic *Pax6*(*5a*) could induce well differentiated retina in chick, replacement of *Pax6* by *Pax6*(*5a*) in the $Pax6^{5a/5a}$ mutants failed to correct the retinal differentiation observed in the *Pax6*-null mutant. Together with the lens development failure in our mutants, these results showed that canonical *Pax6* was uniquely required for mammalian eye development.

Although *Pax2* and *Pax6*(*5a*) failed to reverse *Pax6* homozygous null ocular defects, our studies showed that they could partially replace *Pax6* for telencephalon and neural tube development. In the $Pax6^{5a/5a}$ and $Pax6^{Pax2/Pax2}$ mutants, we showed that *Ngn2* expression was reactivated in dorsal telencephalon, and Nkx2.2 was indeed suppressed in ventral neural tube. Thus, contrary to the previous gain-of-function studies that indicated that *Pax6*(*5a*) only affected cell proliferation in telencephalon, our genetic knock-in experiments supported that *Pax6*(*5a*) could complement *Pax6* in neural patterning and differentiation. In brain development, *Pax6*, *Pax6*(*5a*), and *Pax2* likely share a common set of downstream neurogenesis genes recognizable by their PDs. This is because even Pax2, which lacks a functional HD, could rescue *Ngn2* and Nkx2.2 expression in the $Pax6^{Pax2/Pax2}$ mutants. On the other hand, *Pax6*(*5a*) and *Pax2* were still unable to activate *Sfrp2* at the dorsoventral boundary, consistent with the previous reports that *Sfrp2* regulation required both the PD and the HD of *Pax6* (26, 53). Furthermore, we were able to identify an evolutionarily conserved binding site for the *Pax6*(*5a*) PD in the *Ngn2* telencephalic enhancer and showed that the *in vitro* binding affinities of *Pax6*(*5a*) and *Pax2* PD correlate well with the *Ngn2* expression level. Therefore, at least for *Ngn2*, the strength of the PD binding dictates the functional activity of *Pax6*, *Pax6*(*5a*), and *Pax2 in vivo*.

The diversification of the ancestral *Pax* gene into *Pax6*, *Pax6*(*5a*), and *Pax2* accompanied the arise of sophisticated vision systems in both invertebrates and vertebrates. We have shown that although *Pax6*, *Pax6*(*5a*), and *Pax2* are partially interchangeable in brain development where their HDs are dispensable, *Pax6*(*5a*) and *Pax2* cannot substitute for *Pax6* in eye development where PD and HD are both required. This is in contrast with a previous knock-in study of the *Pax2/5/8* subfamily of *Pax* genes that demonstrated the complete functional equivalence between *Pax2* and *Pax5* (54). Most of the previous efforts in determining *Pax6* downstream targets have focused on its well characterized PD binding site. Our gene replacement studies suggest that it is essential to study the combinatorial activities of PD and HD to understand the unique function of *Pax6* in neural development.

Acknowledgments—We thank Dr. James Li for the $Pax6^{Sey\text{-}Neu/Sey\text{-}Neu}$ *mice and Drs. Lin Gan, Tom Glaser, Jane E. Johnson, Alexandra Joyner, Richard Maas, Andrew McMahon, Milan Jamrich, and Valerie Wallace for reagents.*

REFERENCES

1. Kozmik, Z. (2005) Pax genes in eye development and evolution. *Curr. Opin. Genet. Dev.* **15,** 430–438
2. Fu, W., and Noll, M. (1997) The Pax2 homolog sparkling is required for development of cone and pigment cells in the *Drosophila* eye. *Genes Dev.* **11,** 2066–2078
3. Quiring, R., Walldorf, U., Kloter, U., and Gehring, W. J. (1994) Homology of the eyeless gene of *Drosophila* to the Small eye gene in mice and Aniridia in humans. *Science* **265,** 785–789
4. Jang, C. C., Chao, J. L., Jones, N., Yao, L. C., Bessarab, D. A., Kuo, Y. M., Jun, S., Desplan, C., Beckendorf, S. K., and Sun, Y. H. (2003) Two Pax genes, eye gone and eyeless, act cooperatively in promoting *Drosophila* eye development. *Development* **130,** 2939–2951
5. Dominguez, M., Ferres-Marco, D., Gutierrez-Aviño, F. J., Speicher, S. A., and Beneyto, M. (2004) Growth and specification of the eye are controlled independently by Eyegone and Eyeless in *Drosophila melanogaster*. *Nat. Genet.* **36,** 31–39
6. Punzo, C., Kurata, S., and Gehring, W. J. (2001) The eyeless homeodomain is dispensable for eye development in *Drosophila*. *Genes Dev.* **15,** 1716–1723
7. Azuma, N., Tadokoro, K., Asaka, A., Yamada, M., Yamaguchi, Y., Handa, H., Matsushima, S., Watanabe, T., Kohsaka, S., Kida, Y., Shiraishi, T., Ogura, T., Shimamura, K., and Nakafuku, M. (2005) The Pax6 isoform bearing an alternative spliced exon promotes the development of the neural retinal structure. *Hum. Mol. Genet.* **14,** 735–745

8. Glaser, T., Walton, D. S., and Maas, R. L. (1992) Genomic structure, evolutionary conservation and aniridia mutations in the human PAX6 gene. *Nat. Genet.* **2,** 232–239
9. Grindley, J. C., Davidson, D. R., and Hill, R. E. (1995) The role of Pax-6 in eye and nasal development. *Development* **121,** 1433–1442
10. Hill, R. E., Favor, J., Hogan, B. L., Ton, C. C., Saunders, G. F., Hanson, I. M., Prosser, J., Jordan, T., Hastie, N. D., and van Heyningen, V. (1991) Mouse small eye results from mutations in a paired-like homeobox-containing gene. *Nature* **354,** 522–525
11. Jordan, T., Hanson, I., Zaletayev, D., Hodgson, S., Prosser, J., Seawright, A., Hastie, N., and van Heyningen, V. (1992) The human PAX6 gene is mutated in two patients with aniridia. *Nat. Genet.* **1,** 328–332
12. Ashery-Padan, R., Marquardt, T., Zhou, X., and Gruss, P. (2000) Pax6 activity in the lens primordium is required for lens formation and for correct placement of a single retina in the eye. *Genes Dev.* **14,** 2701–2711
13. Shaham, O., Smith, A. N., Robinson, M. L., Taketo, M. M., Lang, R. A., and Ashery-Padan, R. (2009) Pax6 is essential for lens fiber cell differentiation. *Development* **136,** 2567–2578
14. Marquardt, T., Ashery-Padan, R., Andrejewski, N., Scardigli, R., Guillemot, F., and Gruss, P. (2001) Pax6 is required for the multipotent state of retinal progenitor cells. *Cell* **105,** 43–55
15. Oron-Karni, V., Farhy, C., Elgart, M., Marquardt, T., Remizova, L., Yaron, O., Xie, Q., Cvekl, A., and Ashery-Padan, R. (2008) Dual requirement for Pax6 in retinal progenitor cells. *Development* **135,** 4037–4047
16. Philips, G. T., Stair, C. N., Young Lee, H., Wroblewski, E., Berberoglu, M. A., Brown, N. L., and Mastick, G. S. (2005) Precocious retinal neurons: Pax6 controls timing of differentiation and determination of cell type. *Dev. Biol.* **279,** 308–321
17. Ericson, J., Rashbass, P., Schedl, A., Brenner-Morton, S., Kawakami, A., van Heyningen, V., Jessell, T. M., and Briscoe, J. (1997) Pax6 controls progenitor cell identity and neuronal fate in response to graded Shh signaling. *Cell* **90,** 169–180
18. Stoykova, A., Fritsch, R., Walther, C., and Gruss, P. (1996) Forebrain patterning defects in Small eye mutant mice. *Development* **122,** 3453–3465
19. Chapouton, P., Gärtner, A., and Götz, M. (1999) The role of Pax6 in restricting cell migration between developing cortex and basal ganglia. *Development* **126,** 5569–5579
20. Nomura, T., and Osumi, N. (2004) Misrouting of mitral cell progenitors in the Pax6/small eye rat telencephalon. *Development* **131,** 787–796
21. Carić, D., Gooday, D., Hill, R. E., McConnell, S. K., and Price, D. J. (1997) Determination of the migratory capacity of embryonic cortical cells lacking the transcription factor Pax-6. *Development* **124,** 5087–5096
22. Estivill-Torrus, G., Pearson, H., van Heyningen, V., Price, D. J., and Rashbass, P. (2002) Pax6 is required to regulate the cell cycle and the rate of progression from symmetrical to asymmetrical division in mammalian cortical progenitors. *Development* **129,** 455–466
23. Götz, M., Stoykova, A., and Gruss, P. (1998) Pax6 controls radial glia differentiation in the cerebral cortex. *Neuron* **21,** 1031–1044
24. Epstein, J. A., Glaser, T., Cai, J., Jepeal, L., Walton, D. S., and Maas, R. L. (1994) Two independent and interactive DNA-binding subdomains of the Pax6 paired domain are regulated by alternative splicing. *Genes Dev.* **8,** 2022–2034
25. Mikkola, I., Bruun, J. A., Holm, T., and Johansen, T. (2001) Superactivation of Pax6-mediated transactivation from paired domain-binding sites by DNA-independent recruitment of different homeodomain proteins. *J. Biol. Chem.* **276,** 4109–4118
26. Haubst, N., Berger, J., Radjendirane, V., Graw, J., Favor, J., Saunders, G. F., Stoykova, A., and Götz, M. (2004) Molecular dissection of Pax6 function: the specific roles of the paired domain and homeodomain in brain development. *Development* **131,** 6131–6140
27. Singh, S., Mishra, R., Arango, N. A., Deng, J. M., Behringer, R. R., and Saunders, G. F. (2002) Iris hypoplasia in mice that lack the alternatively spliced Pax6(5a) isoform. *Proc. Natl. Acad. Sci. U.S.A.* **99,** 6812–6815
28. Berger, J., Berger, S., Tuoc, T. C., D'Amelio, M., Cecconi, F., Gorski, J. A., Jones, K. R., Gruss, P., and Stoykova, A. (2007) Conditional activation of Pax6 in the developing cortex of transgenic mice causes progenitor apoptosis. *Development* **134,** 1311–1322
29. Lang, D., Powell, S. K., Plummer, R. S., Young, K. P., and Ruggeri, B. A. (2007) PAX genes: roles in development, pathophysiology, and cancer. *Biochem. Pharmacol.* **73,** 1–14
30. Epstein, J., Cai, J., Glaser, T., Jepeal, L., and Maas, R. (1994) Identification of a Pax paired domain recognition sequence and evidence for DNA-dependent conformational changes. *J. Biol. Chem.* **269,** 8355–8361
31. Bäumer, N., Marquardt, T., Stoykova, A., Spieler, D., Treichel, D., Ashery-Padan, R., and Gruss, P. (2003) Retinal pigmented epithelium determination requires the redundant activities of Pax2 and Pax6. *Development* **130,** 2903–2915
32. Bharti, K., Gasper, M., Ou, J., Brucato, M., Clore-Gronenborn, K., Pickel, J., and Arnheiter, H. (2012) A regulatory loop involving PAX6, MITF, and WNT signaling controls retinal pigment epithelium development. *PLoS Genet.* **8,** e1002757
33. Schwarz, M., Cecconi, F., Bernier, G., Andrejewski, N., Kammandel, B., Wagner, M., and Gruss, P. (2000) Spatial specification of mammalian eye territories by reciprocal transcriptional repression of Pax2 and Pax6. *Development* **127,** 4325–4334
34. Carbe, C., Hertzler-Schaefer, K., and Zhang, X. (2012) The functional role of the Meis/Prep-binding elements in Pax6 locus during pancreas and eye development. *Dev. Biol.* **363,** 320–329
35. Liu, P., Jenkins, N. A., and Copeland, N. G. (2003) A highly efficient recombineering-based method for generating conditional knockout mutations. *Genome Res.* **13,** 476–484
36. Glaser, T., Jepeal, L., Edwards, J. G., Young, S. R., Favor, J., and Maas, R. L. (1994) PAX6 gene dosage effect in a family with congenital cataracts, aniridia, anophthalmia and central nervous system defects. *Nat. Genet.* **7,** 463–471
37. Pan, Y., Carbe, C., Powers, A., Feng, G. S., and Zhang, X. (2010) Sprouty2-modulated Kras signaling rescues Shp2 deficiency during lens and lacrimal gland development. *Development* **137,** 1085–1093
38. Pan, Y., Carbe, C., Powers, A., Zhang, E. E., Esko, J. D., Grobe, K., Feng, G. S., and Zhang, X. (2008) Bud specific N-sulfation of heparan sulfate regulates Shp2-dependent FGF signaling during lacrimal gland induction. *Development* **135,** 301–310
39. Pan, Y., Woodbury, A., Esko, J. D., Grobe, K., and Zhang, X. (2006) Heparan sulfate biosynthetic gene Ndst1 is required for FGF signaling in early lens development. *Development* **133,** 4933–4944
40. Schmahl, W., Knoedlseder, M., Favor, J., and Davidson, D. (1993) Defects of neuronal migration and the pathogenesis of cortical malformations are associated with Small eye (Sey) in the mouse, a point mutation at the Pax-6-locus. *Acta Neuropathol.* **86,** 126–135
41. Guénette, S., Chang, Y., Hiesberger, T., Richardson, J. A., Eckman, C. B., Eckman, E. A., Hammer, R. E., and Herz, J. (2006) Essential roles for the FE65 amyloid precursor protein-interacting proteins in brain development. *EMBO J.* **25,** 420–431
42. Zhang, X., Rowan, S., Yue, Y., Heaney, S., Pan, Y., Brendolan, A., Selleri, L., and Maas, R. L. (2006) Pax6 is regulated by Meis and Pbx homeoproteins during pancreatic development. *Dev. Biol.* **300,** 748–757
43. Zhang, X., Friedman, A., Heaney, S., Purcell, P., and Maas, R. L. (2002) Meis homeoproteins directly regulate Pax6 during vertebrate lens morphogenesis. *Genes Dev.* **16,** 2097–2107
44. Scardigli, R., Bäumer, N., Gruss, P., Guillemot, F., and Le Roux, I. (2003) Direct and concentration-dependent regulation of the proneural gene Neurogenin2 by Pax6. *Development* **130,** 3269–3281
45. Brownell, I., Dirksen, M., and Jamrich, M. (2000) Forkhead Foxe3 maps to the dysgenetic lens locus and is critical in lens development and differentiation. *Genesis* **27,** 81–93
46. Makarenkova, H. P., Ito, M., Govindarajan, V., Faber, S. C., Sun, L., McMahon, G., Overbeek, P. A., and Lang, R. A. (2000) FGF10 is an inducer and Pax6 a competence factor for lacrimal gland development. *Development* **127,** 2563–2572
47. Brown, N. L., Kanekar, S., Vetter, M. L., Tucker, P. K., Gemza, D. L., and Glaser, T. (1998) Math5 encodes a murine basic helix-loop-helix transcription factor expressed during early stages of retinal neurogenesis. *Development* **125,** 4821–4833
48. Briscoe, J., Sussel, L., Serup, P., Hartigan-O'Connor, D., Jessell, T. M., Rubenstein, J. L., and Ericson, J. (1999) Homeobox gene Nkx2.2 and specification of neuronal identity by graded Sonic hedgehog signalling. *Nature*

398, 622–627
49. Aota, S., Nakajima, N., Sakamoto, R., Watanabe, S., Ibaraki, N., and Okazaki, K. (2003) Pax6 autoregulation mediated by direct interaction of Pax6 protein with the head surface ectoderm-specific enhancer of the mouse Pax6 gene. *Dev. Biol.* **257,** 1–13
50. Donner, A. L., Ko, F., Episkopou, V., and Maas, R. L. (2007) Pax6 is misexpressed in Sox1 null lens fiber cells. *Gene Expr. Patterns* **7,** 606–613
51. Rowan, S., Siggers, T., Lachke, S. A., Yue, Y., Bulyk, M. L., and Maas, R. L. (2010) Precise temporal control of the eye regulatory gene Pax6 via enhancer-binding site affinity. *Genes Dev.* **24,** 980–985
52. Favor, J., Peters, H., Hermann, T., Schmahl, W., Chatterjee, B., Neuhäuser-Klaus, A., and Sandulache, R. (2001) Molecular characterization of Pax6(2Neu) through Pax6(10Neu): an extension of the Pax6 allelic series and the identification of two possible hypomorph alleles in the mouse *Mus musculus*. *Genetics* **159,** 1689–1700
53. Kim, A. S., Anderson, S. A., Rubenstein, J. L., Lowenstein, D. H., and Pleasure, S. J. (2001) Pax-6 regulates expression of SFRP-2 and Wnt-7b in the developing CNS. *J. Neurosci.* **21,** RC132
54. Bouchard, M., Pfeffer, P., and Busslinger, M. (2000) Functional equivalence of the transcription factors Pax2 and Pax5 in mouse development. *Development* **127,** 3703–3713